Письма в ЭЧАЯ. 2015. Т. 12, № 6(197). С. 1182–1195

PERSPECTIVES OF STUDY OF THE DIRECT PHOTON PRODUCTION PROCESS AT FAIR ENERGY

A. N. Skachkova [1], *N. B. Skachkov* [2]

Joint Institute for Nuclear Research, Dubna

The modeling of high-energy photon production in collisions of antiproton beam having $E_{\rm beam} = 15$ GeV with the proton target, $\bar{p}p \to \gamma + X$, is done using the event sample simulated by the PYTHIA6 generator. Such an energy is high enough to consider this collision as a relativistic one and being caused by parton–parton scattering. The distribution of the set of kinematic variables and cuts which can be useful for getting the information about proton structure in the available kinematic region is obtained. The contributions of fake photons which can appear from the hadron decays as well as of the background caused by the minimum bias events and other QCD processes are estimated. A set of cuts which can be useful for separation of signal events containing the direct photons from background events is proposed.

Моделирование процесса рождения прямых фотонов в столкновениях антипротонного пучка с протонной мишенью, $\bar{p}p \to \gamma + X$, при энергии пучка, равной 15 ГэВ, выполнено с помощью генератора PYTHIA6. Выбранная энергия является достаточно высокой, чтобы рассматривать столкновения как релятивистские и происходящие путем партон-партонного рассеяния. Получены распределения для набора кинематических переменных, которые важны для получения информации о структуре протона в доступной кинематической области. Даны оценки фонового вклада от несигнальных фотонов, рождающихся в сигнальных событиях при распадах образовавшихся адронов, а также от мини-байесных событий и других непертурбативных процессов. Предложен ряд ограничений, которые могут быть полезны для отделения сигнальных событий, содержащих прямые фотоны, от фоновых событий.

PACS: 13.85.Qk; 07.05.Tp

INTRODUCTION

In Introduction, we review the motivation for study of the processes with direct photon production in hadron–hadron collisions and the development of these processes searches. The measurements of direct photon production in high-energy hadron–hadron interactions have already demonstrated their quite notable potential for studying the structure of hadrons and nuclei. The energy region $1 \leqslant E_{\rm beam} \leqslant 15$ GeV which can be covered by antiproton beam at the accelerator center FAIR (GSI, Darmstadt) is of interest for the research because it is the least investigated as compared to those regions which were studied at the accelerators having

[1] E-mail: Anna.Skachkova@cern.ch
[2] E-mail: nikskach@gmail.com

higher energies. Note that the range $5 \leqslant E_{\rm beam} \leqslant 15$ GeV has all rights to be referred to as a relativistic region of a quite high energy.

In general, the researches at intermediate energies play an important role because in this energy range the methods of the perturbative QCD come into interplay with the rich physics of bound states and resonances. The physics of hadron resonances formation and of their decays is obviously strongly connected with a very important quark confinement problem, i.e., with the parton dynamics at the so-called "large distances". It is clear that the efforts to reach the understanding of the confinement mechanism are of the same great significance as it was, for example, with the discovery of the Higgs boson.

Therefore, a detailed and high-precision study of processes, based on a usage of the experimentally obtained information about the kinematic distributions of detected particles at beam energies available for FAIR, may help to discriminate between a large variety of existing theoretical pertubative and non-perturbative approaches and models that already exist or under development now. It is obvious that high-energy photons (referred to as the "prompt" or "direct" photons) belong to such kind of particles which can bring clear and important information about the processes which we plan to search for.

Of most interest are those prompt photons which are produced directly in the fundamental primary parton–parton collision subprocesses, which initiate the further conversion into the secondary subprocesses of hadronization and emission of stable and unstable particles. The great advantage of direct photons is that they mostly escape these secondary subprocesses. It happens so due to the obvious fact that the photons participate in interactions with other particles only through the electromagnetic interaction coupling constant $\alpha_{\rm em} = 1/137$, which is essentially smaller than the strong coupling constant $\alpha_s(Q^2)$. In the leading order the parton–parton subprocesses with direct photon production, like $q\bar{q} \to \gamma + g$ and $qg \to \gamma + q$, the strong coupling constant governs the interactions of quarks (antiquarks) with the gluons [1] in the same fundamental primary parton–parton collision. It is worth noting that the electromagnetic coupling constant, which defines the radiation of a photon from an electromagnetic charged quark, is very well known, while the measurements of strong coupling constant still go on.

Now some words about the development of direct photon physics. The study of direct photon production in hadron–hadron collisions was preceded by the study of the production of light elementary particles, mainly the mesons, like π^0, η and ω. The production of photons from proton–proton (pp) collisions has been the object of many experimental measurements done both at FNAL [1] and at the ISR (CERN).

It should be mentioned that at the same time, no systematic investigations concerning the source of the observed photons have been made and it has been commonly assumed that these photons are produced through the π^0 and η decays. Nevertheless, it was noted in [1] that the differential cross sections of the process $p + p \to \gamma + X$ (X is "*anything*"), measured in the range of P_T from 0.2 to 3 GeV/c, have shown a significant deviation from the widely used simple exponential behavior in P_T for incident proton energies above 50 GeV and P_T greater than 1 GeV/c.

Later the collaboration R412 at the ISR [2] (see also [3]) made a presentation on the first observation of large production of signal photons (and also photon pairs), in an analogous

[1] They can further take part in the secondary subprocesses which include the interactions with the "underlying partons", which have not participated in the fundamental subprocess.

transverse momentum range (1.6 to 3.8 GeV/c), which cannot be explained by π^0 and η decays. After this discovery, the results of the subsequent analogous pioneering experiments were presenting, almost every year, new arguments in favor of the production of direct photons and the information about the properties of such processes (for more information, see [4–6]).

To date there is a lot of new interesting information about direct photon production which came from high-energy colliders. Thus, the Tevatron and LHC (for the recent results, see, for example, [7–10], which contain the corresponding references) have provided the information about the behavior of cross sections of nucleons collision in a region of large transverse momenta. This information is important for the further development of perturbative QCD at high energies. Also very important results were obtained from study of events with direct photon production in heavy-ion collisions. They have been started at CERN SPS (see [11]) and up to date continue in recent measurements at BNL [1]. These measurements have shown that the processes with direct photon production play the crucial role in search and study of Quark–Gluon Plasma.

Meanwhile, in practice, there was not so much progress reached in studying the processes with direct photon production in the region of intermediate beam energy which is important for search of expected deviations from the perturbative QCD. The measurement of direct photon production can provide new information about the behavior of proton structure function in the desired intermediate energy region.

The aim of the present paper is to make an estimation of the distributions of the most important kinematical variables of: 1) the produced direct photons and 2) the fake photons. We use the PYTHIA6.4 generator [12] which includes only those events which are defined by the leading order (LO) subprocesses $q\bar{q} \to \gamma + g$ and $qg \to \gamma + q$. In the following, these events will be called "signal events", and the photons produced in this subprocess will be called "signal photons". The fake photons which are produced in hadron (mainly mesons) decays in the same signal event will be called "decay photons". The leading order CTEQ3L parametrization was used which is known to be quite useful for the intermediate energies.

Section 1 contains the kinematical distributions obtained for the single direct photons and the estimation of the size of the kinematic region available for the measurement of the parton distribution functions (PDFs).

The important problem for the planned measurements is connected with the presence of background. Sections 2 and 3 are devoted to the estimation of the background contribution. Section 2 is focused on the background photons which appear in the signal events containing the direct photons. The introductory part of this section includes the plots which provide the information about the size of the background contribution coming from the parent particles of fake photons and also from their grandparents the connections of which are based on the LUND [12] fragmentation model. Subsection 2.1 contains the plots showing the kinematical and other distributions of neutral pions which are the major source of background. Subsection 2.2 presents the plots with the kinematical distributions of the fake photons and the plots with the distributions, which show the position of fake photon production vertices in signal events, as well as the plot giving the information about distribution of the numbers of fake photons per signal events. In Subsec. 2.3 we discuss the criteria that can be useful for background separation in signal events having the direct photons.

[1] See 1) PHENIX: arxiv:1205.0206 and 2) STAR: arxiv:1201.3093.

Section 3 is devoted to a much more difficult background which appears when the non-perturbative minimum-bias processes and the other than the signal events are taken into account. This section contains the values of the cross sections, predicted by PYTHIA6.4 for the case of antiproton beam having $E_{\rm beam} = 15$ GeV, which are significanly higher than the cross section of the signal process $\bar{p}p \to \gamma + X$. The criteria to reduce this background for such processes are proposed. Section 4 contains the Summary.

1. DISTRIBUTIONS OF THE SIGNAL PHOTONS PRODUCED in $p\bar{p}$ COLLISIONS

The sample of 1 000 000 events was generated using three leading order QCD subprocesses $q\bar{q} \to \gamma + g$, $qg \to \gamma + q$ and $gg \to \gamma + g$ which have to be, according to PYTHIA, the candidates for production of direct photons. Table 1 shows the values of their cross sections.

Table 1. **Signal processes and their cross sections**

PYTHIA's number of subprocess	Type of process	Cross section, mb
14	$f + \bar{f} \to g + \gamma$	$1.53 \cdot 10^{-3}$
29	$f + g \to f + \gamma$	$8.18 \cdot 10^{-4}$
115	$g + g \to g + \gamma$	$2.30 \cdot 10^{-7}$

The generated sample allows one to make the plots with the distributions of the most important kinematical physical variables. We consider first the case when no any kinematical cuts are applied. The corresponding distributions are presented in Fig. 1: the signal direct photon energy $E^{\gamma}_{\rm dir}$ (Fig. 1, *a*), its transverse momentum $P^{\gamma}_{T\,\rm dir}$ (Fig. 1, *b*) and the polar angle $\theta^{\gamma}_{\rm dir}$ (Fig. 1, *c*), calculated from the beam direction. Figure 1, *d* shows the distribution of the Bjorken x-variable (it is found that the shapes and top positions of different partons look very similar). Recall that we present here the results which are obtained by PYTHIA for $E_{\rm beam} = 15$ GeV and use the QCD leading order model CTEQ3L the PDF parametrization of which was providing a suitable approximation in the region of intermediate energies. All of these x-distributions cover practically the same region, $0.06 < x < 0.7$, and they have rather similar sharp tops at $x = 0.2$.

The vertical axes in most of the figures (these and the following) show the number of events (per bin) that may be expected per year (10^7 s) for the luminousity $L = 2 \times 10^{32}$ cm$^{-2}\cdot$ s^{-1}. The total number of expected events is shown as the "Integral" values in the statistical frames of the figures.

As can be seen in Fig. 1, *a*, the energy of photons is distributed in a region $0 < E^{\gamma}_{\rm dir} < 12$ GeV. The P_T values range $0 < P^{\gamma}_{T\,\rm dir} < 2.3$ GeV/*c* (Fig. 1, *b*) and the polar angle $\theta^{\gamma}_{\rm dir}$ (Fig. 1, *c*) distribution cover the range of $0 < \theta < 180°$.

The first three plots of Fig. 1 provide important information. First, one can see that the energy distribution has the mid-point at about 3 GeV. It means that about half of direct photons have the energy $E^{\gamma}_{\rm dir} > 3$ GeV. So, they may be considered as quite energetic ones. It is also seen from Fig. 1, *b* that about 35% of photons may have P^{γ}_{T} higher than 1 GeV/*c*, and about 10% of them have P^{γ}_{T} higher than 1.5 GeV/*c*. Figure 1, *c* shows that the mean value of polar angle distribution lies at 27°. It should be noted that switching

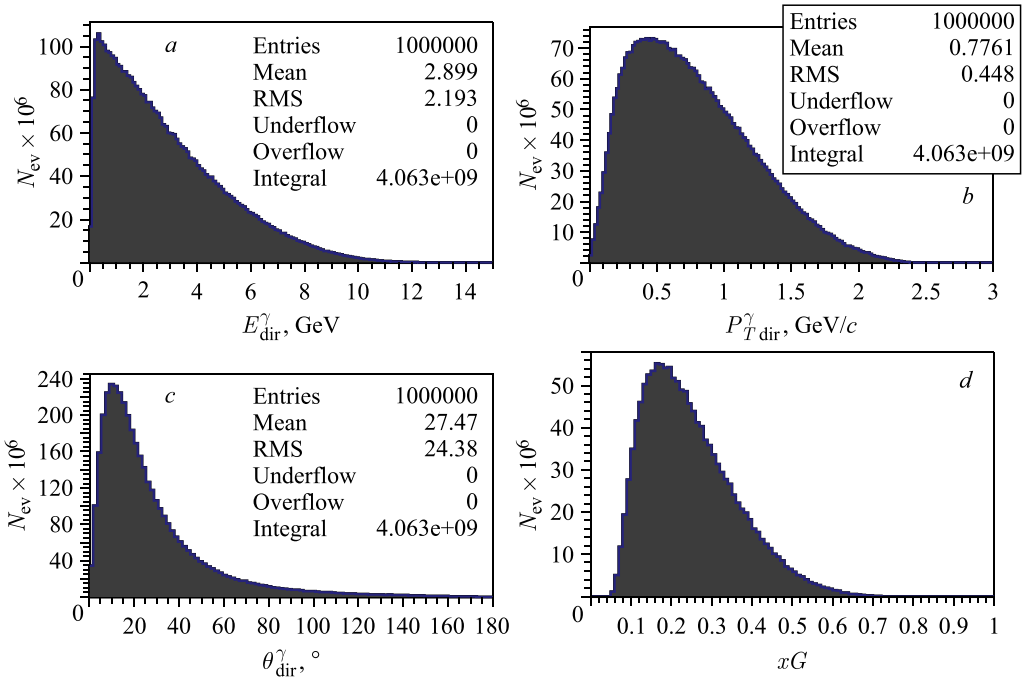

Fig. 1. *a*) Energy $E^{\gamma}_{\rm dir}$; *b*) transverse momentum $P^{\gamma}_{T\,\rm dir}$; *c*) polar angle $\theta^{\gamma}_{\rm dir}$; *d*) x-distributions of partons

"on" and "off" of the initial state radiation does not have a sizable influence on the shape of distributions.

Finally, summarizing the results of Sec. 1, we may conclude that with the beam energy about 15 GeV the proton structure function can be measured in the intervals $0.06 < x < 0.7$ and $0 < Q^2 < 5.3$ GeV^2, where we follow the customary definition of the square of the momentum transferred as $Q^2 = P_T^2$ which is used in the physics of hadron–hadron collisions.

2. FAKE PHOTONS IN SIGNAL EVENTS

The signal events, generated with the $q\bar{q} \to \gamma + g$ and $qg \to \gamma + q$ subprocesses, should also contain some hadrons in the final state. Fortunately, their number would be essentially restricted by the upper limit caused by the beam energy $E_{\rm beam} = 15$ GeV.

This may simplify greatly the identification of final-state particles and the physical analysis due to the reduction of the phase space and, therefore, due to the reduction of the number of hadrons and other particles which may be produced in event directly or in the decay cascades of other hadrons. These hadrons may decay within the detector volume and thus produce the background photons which may fake the signal ones, produced in signal annihilation subprocesses. Here, we use PYTHIA event generator option for getting the information about the parent particles, which serve as the origin of the outgoing decay products. Figure 2 contains two plots which show the size of contributions of these parents and grandparents of fake photons.

Figure 2, *a* presents the contribution of different parent particles to the processes of fake photon creation in signal reactions. It clearly demonstrates that among all of the shown sources of fake photons (see Table 2) the contribution of neutral pion π^0 decay (bin 1,

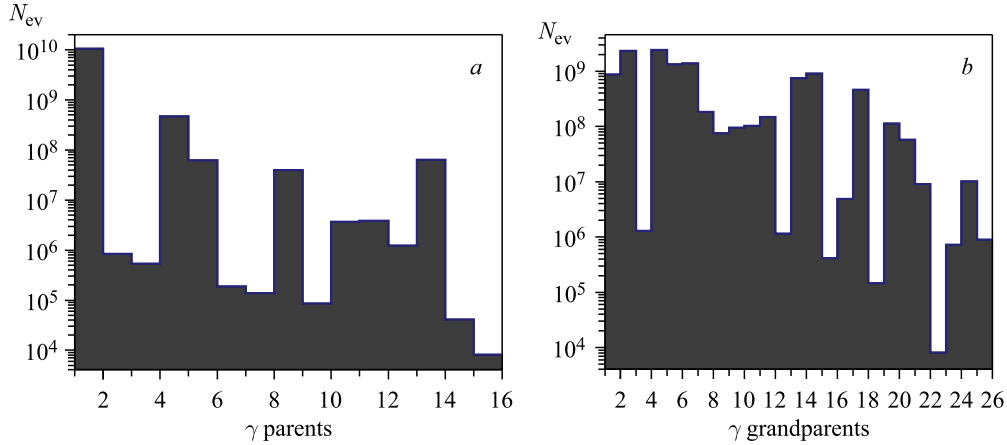

Fig. 2. Contributions (in the signal events) of: *a*) the parents of fake γ's; *b*) the grandparents of fake γ's

Table 2. **Bin correspondence to the particle names for the case of γ parents and grandparents**

Bin number	Name of γ parent particle	Name of γ grandparent particle
1	π^0	Cluster
2	ρ^0	String
3	ρ^+	ρ^0
4	η	ρ^+
5	ω	η
6	K^{*0}	ω
7	K^{*+}	K_S^0
8	η'	K^{*0}
9	ϕ	K^+
10	Δ^0	K^{*+}
11	Δ^+	η'
12	Λ^0	ϕ
13	Σ^0	Δ^0
14	Σ^+	Δ^+
15	Ξ^0	p
16		Σ^{*-}
17		Λ^0
18		Σ^0
19		Σ^{*0}
20		Σ^+
21		Σ^{*+}
22		Ξ^-
23		Ξ^{*-}
24		Ξ^0
25		Ξ^{*0}

Table 2) is a dominant one. It provides a much higher (more than one order) contribution than all of the other decay channels. The next contribution, which is more than about one order less, comes from the η (bin 4, Table 2), and then follow, in decending order, the decays of ω (bin 5, Table 2), Σ^0 (bin 13, Table 2), η' (bin 8, Table 2) and of other mesons.

Figure 2, *b* shows an analogous distribution of a number of background photons versus the type of their grandparents. The correspondence between the bin numbers shown on the x axis of Figs. 2, *a* and *b* and the names of the parent and grandparent particles can be found by using Table 2.

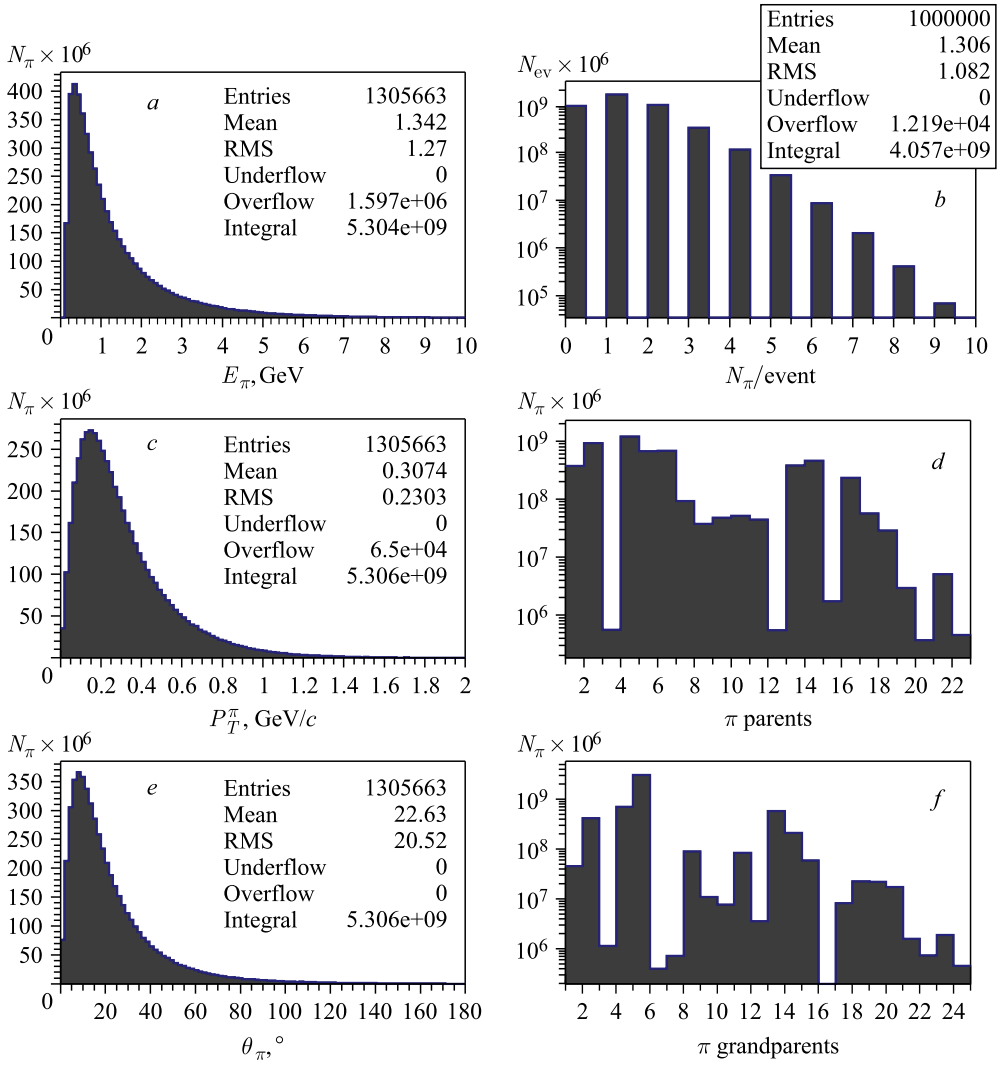

Fig. 3. Contributions (in the signal events) of: left column — distributions of the number of neutral pions versus: *a*) energy E_π; *c*) transverse momentum P_T^π; *e*) polar angle θ_π; right column — distributions of: *b*) the total number of pions N_π per event; *d*) number of specified parent particles for pions; *f*) number of grandparent particles for pions

To get the idea about the role of the "parent particles", it is natural to look first for the case of neutral pions which give a dominant contribution to the background. These pions, as will be discussed in the following subsection, may arise from decays of η and ω mesons or more heavier mesons and baryons, which are produced as the resonance states according to the LUND fragmentation model.

2.1. Pions in Signal Events. The distributions of the kinematical variables of neutral pions, which are produced in the same sample of signal events, are presented in Fig. 3.

Figures 3, *a, c* and *e* show the pions energy, transverse momentum and polar angle distributions, respectively. As seen from Fig. 3, *a*, the pions energy covers the range of $0 \leqslant E_\pi \leqslant 7$ GeV and it has the average value $\langle E_\pi \rangle = 1.3$ GeV. The transverse momenta of these pions (Fig. 3, *c*) cover the range $0 \leqslant P_T^\pi \leqslant 1.4$ GeV/*c* and their average value is about $\langle P_T^\pi \rangle = 0.3$ GeV/*c*.

It is seen from the statistical frame that the number of produced neutral pions is about 13% higher than the number of generated signal events with the direct photons. Figure 3, *b* provides the distribution of the number of pions per event (N_π/event). It is worth noting that the first bin of the logarithmic vertical axis shows that quite a sizable part of events do not have at all the pions in the final state. Nevertheless, Fig. 3, *b* also demonstrates that there can appear some signal events (with the direct photons) which have up to nine pions.

Table 3. **Bin correspondence to the particle names for the case of π^0 parents and grandparents**

Bin number	Name of π^0 parent particle	Name of π^0 grandparent particle
1	Cluster	d quark
2	String	u quark
3	ρ^0	s quark
4	ρ^+	Cluster
5	η	String
6	ω	ρ^0
7	K_S^0	ω
8	K^{*0}	K^0
9	K^+	K^{*0}
10	K^{*+}	K^{*+}
11	η'	η'
12	ϕ	ϕ
13	Δ^0	ud diquark, $S = 0$
14	Δ^+	ud diquark, $S = 1$
15	Σ^{*-}	uu diquark, $S = 1$
16	Λ^0	Neutron
17	Σ^{*0}	Σ^{*-}
18	Σ^+	Σ^-
19	Σ^{*+}	Σ^{*0}
20	Ξ^{*-}	Σ^{*+}
21	Ξ^0	Ξ^-
22	Ξ^{*0}	Ξ^{*-}
23		Ξ^0
24		Ξ^{*0}

Figures 3, *d* and *f* show, by using Table 3, the contributions of pion parent and grandparent particles, correspondingly. Table 3 presents the bin numbers used to numerate the parents and grandparents of π^0's, as was done previously in Table 2, for numeration of parents and grandparents sources of fake photons which are produced in the signal events. These plots show that the main sources of π^0 production are: the "strings", ρ^+, η, ω, $\Delta^{0(+)}$ and "cluster". These distributions would be useful for distinguishing of fake photons.

2.2. The Kinematical Distributions of Background Photons in Signal Events. The main kinematical distributions of background photons in signal events are presented in Fig. 4. They

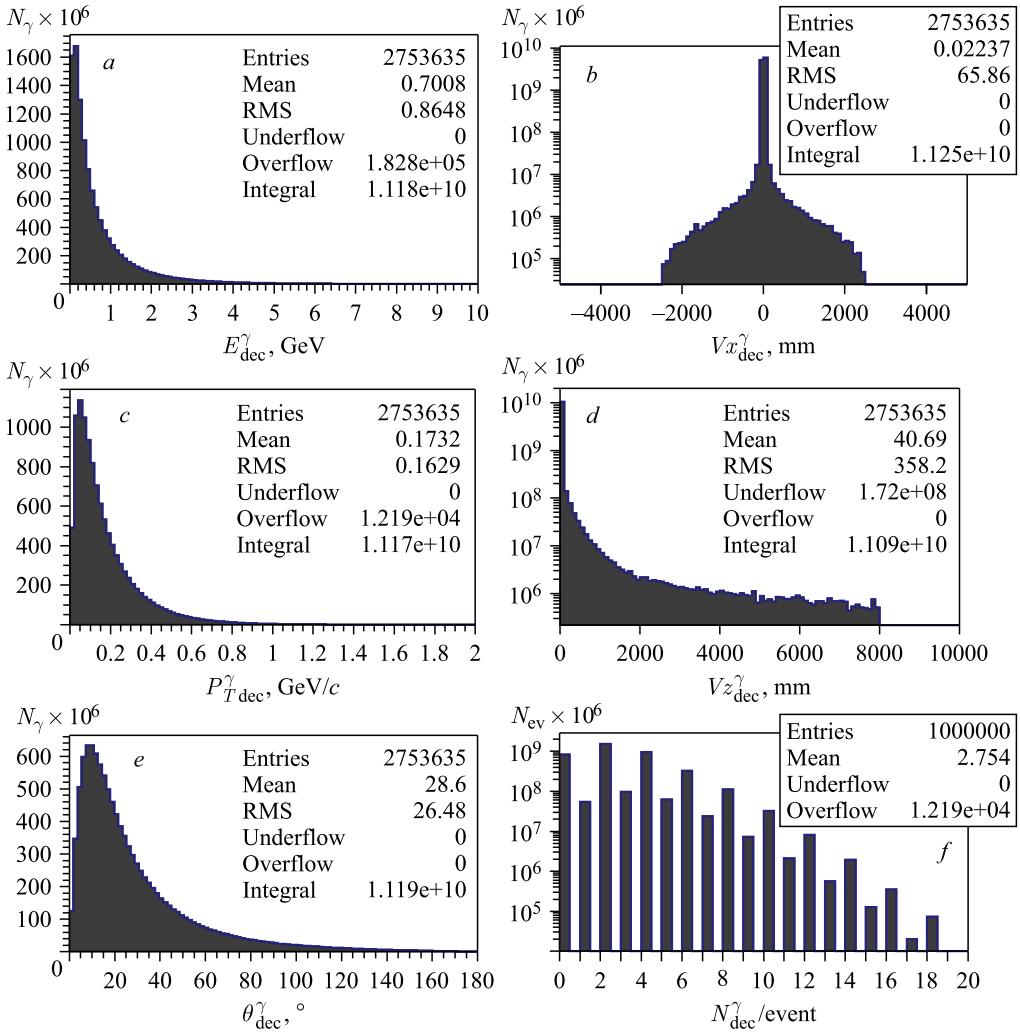

Fig. 4. Left column — distributions of the number of fake photons versus their: *a*) energy $E^\gamma_{\rm dec}$; *c*) transverse momentum $P^\gamma_{T\,\rm dec}$; *e*) polar angle $\theta^\gamma_{\rm dec}$. Right column — distributions of: *b*) x coordinate of fake γ production vertex; *d*) z coordinate of fake γ production vertex; *f*) the total number $N^\gamma_{\rm dec}$ of fake photons per signal event

are obtained using the same sample of one million signal events which was used in Sec. 1 and Subsec. 2.1.

One can see from the statistics frame in the upper part of the plots that the contribution of all of the fake photons, including the contribution from the neutral pions which was discussed before, can be larger by a factor of about 2.75 than the number of signal direct photons.

From Fig. 4, *a* one can see that the energy of the fake photons covers the range $0 \leqslant E^{\gamma}_{\rm dec} \leqslant 5$ GeV and it has the average value $\langle E^{\gamma}_{\rm dec} \rangle = 0.7$ GeV. At the same time, the range of the transverse momentum (Fig. 4, *c*) is $0 \leqslant P^{\gamma}_{T\,\rm dec} \leqslant 1$ GeV/*c* and it has the average value $\langle P^{\gamma}_{T\,\rm dec} \rangle = 0.17$ GeV/*c*.

The comparison of the plots shown in Fig. 4 for the energy $E^{\gamma}_{\rm dec}$ and the transverse momentum $P^{\gamma}_{T\,\rm dec}$ distributions of fake photons with the analogous plots *a* and *b* in Fig. 1 for signal photons shows that they are very different (by a factor of approximately 3), while the angle distributions in Fig. 1, *c* and Fig. 4, *e* have practically the same shapes. Both of them cover practically the same range $0 \leqslant \theta^{\gamma} \leqslant 180^{\circ}$ and have the average value of about $\langle \theta^{\gamma} \rangle = 28^{\circ}$.

One can see from the shapes of the $P^{\gamma}_{T\,\rm dec}$ distribution of fake photons, shown in the plot *c* of Fig. 4 and in the corresponding plot *b* for direct photons in Fig. 1, that the cut of about $P^{\gamma}_{T} > 0.77$ GeV/*c* may allow one to eliminate the fake photons at the cost of a bit less than half of signal direct photons loss.

The right-hand column of Fig. 4 includes the plots *b* and *d* which contain the values of the Vx (Vy distribution is identical to that one of Vx) and Vz components of the 3-vector $\mathbf{V}$ which points the position (in mm) of fake photon production vertex. The logarithmic scales of Vx and Vz axes show that most fake photons in the signal events are produced very close to the point of direct photon production (interaction point).

Figure 4, *f* shows the spectrum of the number of fake photons per event (analogously to Fig. 3, *b* for the number of neutral pions). It is seen that the number of signal events which do not have fake photons at all (bin 0) is quite large and the range of the number of fake photons in event ($N^{\gamma}_{\rm dec}$/event) grows up by a factor of 2 and it spreads up to 18: $0 < N^{\gamma}_{\rm dec}/{\rm event} < 18$.

2.3. Separation of Background Photons in Signal Events. To reduce the fake photon background, we propose the next two selection cuts:

1) Gamma isolation criteria. We select only those photons for which the summed energy $E_{\rm sum}$ of all the charged particles around the photon within the cone of the radius $R = \sqrt{\Delta^2_{\varphi} + \Delta^2_{\eta}} = 0.2$ in the $\eta - \varphi$ space is less than 0.25 GeV, i.e., $E_{\rm sum} \leqslant 0.25$ GeV [1].

2) Restriction on photon P^{γ}_{T}. We select only those photons which have the transverse momentum higher than 0.2 GeV/*c*, i.e., $P^{\gamma}_{T} \geqslant 0.2$ GeV/*c*.

The plots presented in Fig. 5 illustrate the action of the photon isolation criterion used for the definition of the first cut. They show the distributions of the total energy of the charged particles which are contained within the cones of the radius R around the photon direction of the momentum. The comparison of the plot *a* (for the signal photons) with the plot *b* (for the

[1] Here $\Delta_{\varphi} = \varphi_{\gamma} - \varphi_{p}$ is the difference of the photon's (γ) azimuth angle φ_{γ} and the azimuth angle φ_{p} of the particle (p). Analogously, $\Delta_{\eta} = \eta_{\gamma} - \eta_{p}$ is the difference of the photon and the particle pseudorapidities. The azimuth angle φ and the polar (zenith) angle θ (counted from the beam direction) are used to determine the direction of particle 3-momentum. The particle pseudorapidity η is defined as $\eta = -\ln \tan(\theta/2)$.

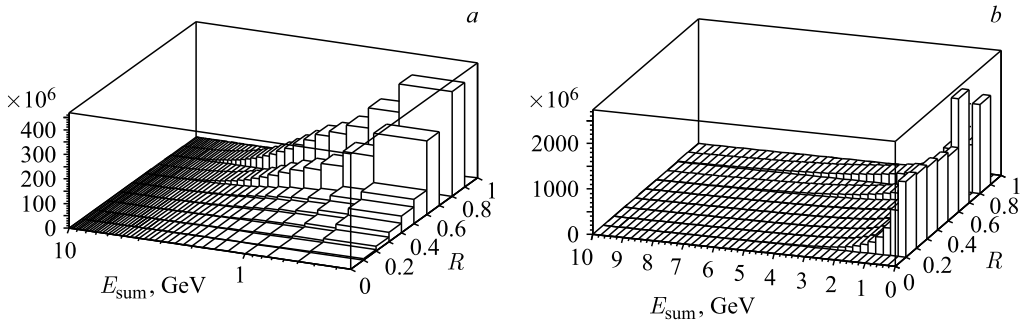

Fig. 5. Demonstration of photon isolation criterion. Distributions of the summed energy $E_{\rm sum}$ within the cone of the radius $R = 0.1, 0.2, 0.3\ldots$ around: *a*) signal photons; *b*) background photons

background photons) shows that the signal photons have much smaller summarized energy content within the cone of $R \leqslant 0.2$ than the energy content around the fake photons. The choice of the values $E_{\rm sum} \leqslant 0.25$ GeV within $R = 0.2$ allows one to minimize the number of background fake photons by 67%, with the 1.2% loss of signal events.

The second cut $P_T^\gamma \geqslant 0.2$ GeV allows one to reduce the background to 1.3%, thus achieving the signal-to-background ratio $S/B = 73.9$ at the cost of additional loss of 6.5% of signal events. The value of $P_T^\gamma \geqslant 0.25$ GeV/*c* allows one to suppress the fake photons background in signal events completely.

3. BACKGROUND TO THE DIRECT PHOTON PRODUCTION $p\bar{p} \to \gamma + X$

The main contribution to background for the process of direct photon production comes from the processes presented in Table 4 in order of their cross section decrease. As can be seen (by comparison with Table 1), their cross sections are a few orders higher than the signal process cross section. So, it is especially important to find out the criteria for their suppression.

Table 4. **Background processes and their cross sections**

PYTHIA's number of subprocess	Type of process	Cross section, mb
95	Low-P_T scattering	$3.37 \cdot 10^1$
92	Single diffractive (XB)	1.72
93	Single diffractive (AX)	1.72
94	Double diffractive	$2.48 \cdot 10^{-1}$
28	$f + g \to f + g$	$1.67 \cdot 10^{-2}$
68	$g + g \to g + g$	$4.89 \cdot 10^{-3}$
11	$f + f' \to f + f'$ (QCD)	$8.76 \cdot 10^{-3}$
12	$f + \bar{f} \to f' + \bar{f}$	$1.11 \cdot 10^{-3}$
13	$f + \bar{f} \to g + g$	$1.07 \cdot 10^{-3}$
53	$g + g \to f + \bar{f}$	$1.29 \cdot 10^{-4}$

The distributions of the photons from the background events over their energy, transverse momentum, zenith angle and the number of photons per event are presented in Fig. 6. From the plots shown in this figure one can see that the energy of fake photons in the background events is rather low. The distribution of background photons over their energy, see Fig. 6, *a* (they are concentrated mostly in the region less than 2 GeV), covers the range $0 \leqslant E^{\gamma}_{\text{bkg}} \leqslant 4$ GeV and it has the mean value $\langle E^{\gamma}_{\text{bkg}} \rangle = 0.64$ GeV. Analogously, the background photons have low transverse momenta (mostly $P^{\gamma}_{T\,\text{bkg}} < 0.4$ GeV/c with the range $0 \leqslant P^{\gamma}_{T\,\text{bkg}} \leqslant 0.7$ GeV/c and the mean value $\langle P^{\gamma}_{T\,\text{bkg}} \rangle = 0.15$ GeV/c). Figure 6, *b* shows the polar angle distribution for the background photons. It covers the region $0 \leqslant \theta^{\gamma}_{\text{bkg}} \leqslant 180^{\circ}$ and has the mean value $\langle \theta^{\gamma}_{\text{bkg}} \rangle = 30.3^{\circ}$. So, it is very similar to the angle distribution of signal photons shown in Fig. 1, *c*. From Fig. 6, *d* one can see that the background events may include up to 18 photons. Let us note that some (11.2%) of the background processes from Table 4 may not include photons at all (see Fig. 6, *d*, bin 0).

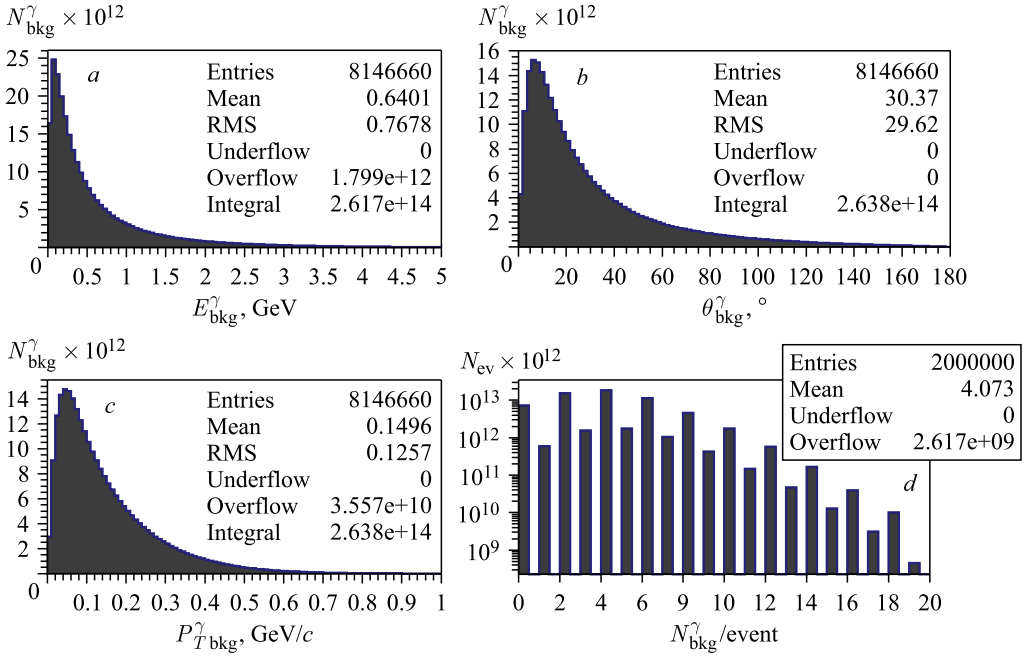

Fig. 6. Left column — distributions of the number of background photons versus their: *a*) energy E^{γ}_{bkg}; *c*) transverse momentum $P^{\gamma}_{T\,\text{bkg}}$. Right column — distributions of: *b*) the polar angle $\theta^{\gamma}_{\text{bkg}}$; *d*) the total number N^{γ}_{bkg} of the photons per the background event

To perform the background suppression, we propose to apply the following two criteria, similar to those used for the signal process case:

1) The isolation criterion for the leading photon (photon with the highest energy in event): we select only those events in which the summed energy of all the charged particles around the leading photon within the cone of the radius $R = \sqrt{\Delta^2_{\varphi} + \Delta^2_{\eta}} = 0.2$ in the $\eta - \varphi$ space is restricted by the relation $E_{\text{sum}} \leqslant 0.25$ GeV. This restriction allows us to exclude 83.7% of background events.

2) The transverse momentum cut on the leading photon is $P_T^\gamma > 0.2$ GeV/c. This criterion allows us to suppress the background down to 4.9%.

The proposed cuts look quite promising for the separation of the signal from the background. The next step which may be done is to take into account the detector effects basing on the GEANT package.

4. SUMMARY

The present paper contains the results of modeling of one of the most important benchmark processes of direct photon production in antiproton–proton collision $\bar{p}p \to \gamma + X$ for the antiproton beam with the energy $E_{\rm beam} = 15$ GeV. The set of kinematical distributions such as the energy, the transverse momentum and the angle of the signal photons was obtained. These distributions show the size of kinematical regions which can be expected for the study. The estimation of the size of the $x{-}Q^2$ kinematical area, which can be available for the measurements of the nucleon structure function at FAIR, is done.

The sources of background which is caused by the presence of the fake photons in the final state of the signal processes are studied in detail. The way to get rid of them was proposed. Two cuts were worked out. They are the "gamma isolation criteria" and the "photon P_T^γ restriction" which allow one to reach a good suppression of the influence of fake photons in the signal events. It was shown that the application of such a method to the case when the background is caused by the other QCD and minimum-bias processes can also help to reach a good background suppression.

Acknowledgements. The work was carried out with the financial support of SAEC "Rosatom" and Helmholtz Association for A. N. Skachkova.

REFERENCES

1. *Carey D. C. et al.* Production of Large-Transverse-Momentum Gamma Rays in pp Collisions for 50 to 400 GeV // Phys. Rev. Lett. 1974. V. 32. P. 24–27.
2. *Darriulat P. et al.* Large Transverse Momentum Photons from High-Energy Proton–Proton Collisions // Nucl. Phys. B. 1976. V. 110. P. 365–379.
3. *Holder M. et al.* High-Resolution Total Absorption Spectrometer for Simultaneous Detector of Several High-Energy Gamma Rays // Nucl. Instr. Meth. 1973. V. 108. P. 541–550.
4. *Aurenche P., Lindfors J.* Direct Photon Production beyond Leading Order in QCD // Nucl. Phys. B. 1980. V. 168. P. 296–314.
5. *Ferbel T., Molzon W. R.* Direct Photon Production in High-Energy Collisions // Rev. Mod. Phys. 1984. V. 56. P. 181–221.
6. *Owens J. F.* Large Momentum Transfer Production of Direct Photons, Jets, and Paricles // Rev. Mod. Phys. 1987. V. 59. P. 465–504.
7. *Abazov V. M. et al. (D0 Collab.).* Measurement of the Differential Cross Section of Photon Plus Jet Production in $p\bar{p}$ Collisions at $\sqrt{s} = 1.96$ TeV // Phys. Rev. D. 2013. V. 88. P. 072008.
8. *Aaltonen T. et al. (CDF Collab.).* Measurement of the Cross Section for Direct Photon Production in Association with a Heavy Quark in $p\bar{p}$ Collisions at $\sqrt{s} = 1.96$ TeV // Phys. Rev. Lett. 2013. V. 111, No. 4. P. 042003.

9. *Chatrchyan S. et al. (CMS Collab.).* Measurement of the Triple-Differential Cross Section for Photon Plus Jets Production in Proton–Proton Collisions at $\sqrt{s} = 7$ TeV // JHEP. 2014. V. 1406. P. 009.
10. *Aad G. et al. (ATLAS Collab.).* Measurement of the Inclusive Isolated Prompt Photons Cross Section in pp Collisions at $\sqrt{s} = 7$ TeV with the ATLAS Detector Using 4.6 fb^{-1} // Phys. Rev. D. 2014. V. 89. P. 052004.
11. *Aggarwal M. M. et al. (WA98 Collab.).* Observation of Direct Photons in Central ^{208}Pb + ^{208}Pb Collisions // Phys. Rev. Lett. 2000. V. 85. P. 3595–3599.
12. *Sjostrand T., Mrenna S., Skands P.* PYTHIA 6.4 Physics and Manual // IOP Science. JHEP. 2006. V. 05. 583 p.

Received on May 23, 2015.